

PROCEEDINGS OF SPIE

[SPIDigitalLibrary.org/conference-proceedings-of-spie](https://spiedigitallibrary.org/conference-proceedings-of-spie)

Developments of scientific CMOS as focal plane detector for Einstein Probe mission

Wang, Wenxin, Ling, Zhixing, Zhang, Chen, Wang, Xinyang, Wu, Qiong, et al.

Wenxin Wang, Zhixing Ling, Chen Zhang, Xinyang Wang, Qiong Wu, Zhenqing Jia, Weimin Yuan, Shuangnan Zhang, "Developments of scientific CMOS as focal plane detector for Einstein Probe mission," Proc. SPIE 10699, Space Telescopes and Instrumentation 2018: Ultraviolet to Gamma Ray, 106995O (6 July 2018); doi: 10.1117/12.2311922

SPIE.

Event: SPIE Astronomical Telescopes + Instrumentation, 2018, Austin, Texas, United States

Developments of scientific CMOS as focal plane detector for Einstein Probe mission

Wenxin Wang^a, Zhixing Ling^{*a}, Chen Zhang^{a,b}, Xinyang Wang^c, Qiong Wu^d, Zhenqing Jia^a, Weimin Yuan^{a,b}, Shuangnan Zhang^{a,e}

^aNational Astronomical Observatories, Chinese Academy of Sciences, Beijing, 100101, China;

^bSchool of Astronomy and Space Science, University of Chinese Academy of Sciences, Beijing, 100049, China; ^cGpixel inc., Changchun, 130033, China; ^dBeijing Weihua High Tech Co.,Ltd., Beijing, 100086, China; ^eInstitute of High Energy Physics, Chinese Academy of Sciences, Beijing, 100049, China

ABSTRACT

China's Einstein Probe (EP) mission is designed for time-domain astrophysics with energy band of 0.5-4 keV. The payloads of EP include a wide-field X-ray telescope (WXT) and a follow-up X-ray telescope (FXT). The field of view (FOV) of WXT is about 3600 square degrees with sensitivity at least 10 times better than traditional X-ray all-sky monitors applying collimators or coded-masks.

Back-side illuminated scientific CMOS (BSI sCMOS) is the best choice for WXT after several types of X-ray detectors are investigated. In this work, we study a BSI sCMOS sensor, GSENSE400BSI developed by Gpixel Inc., which is treated as a pathfinder for the focal plane detector of WXT. GSENSE400BSI has a pixel array of 2048×2048 with pixel size of 11 μm. We have characterized this BSI sCMOS as an X-ray detector. Based on the excellent performance of GSENSE400BSI, a new BSI sCMOS device with large sensitive area of 6×6 cm² has been proposed as the focal plane detector for WXT.

Keywords: Einstein Probe (EP) mission, wide-field X-ray telescope, semiconductor detector, back-side illuminated sCMOS, X-ray detector

1. INTRODUCTION

The Einstein Probe mission is designed for time-domain astronomy in the soft X-ray energy band of 0.5-4 keV and is scheduled to be launched in late 2022. The main payloads of EP are shown in Figure 1. A wide-field X-ray telescope (WXT) onboard EP will be used to discover and locate X-ray transients. The field of view (FOV) of WXT is more than 3600 square degrees which covers one-eleventh of the sky. A lobster-eye type X-ray focusing telescope based on Micro-Pore Optics (MPO)^[1] is employed in WXT, which provides sensitivity at least 10 times better than traditional X-ray all-sky monitors applying collimators or coded-masks. WXT is composed of 12 identical modules, the focal plane of each module is 12.3×12.3 cm². The total imaging spectra focal plane of WXT is more than 1700 cm².

In recent years, complementary metal-oxide-semiconductor (CMOS) devices have been widely applied in optical and infrared applications^[2,3,4]. The features of CMOS devices, such as a high readout frame rate, no charge transfer, good radiation hardness and high circuit integration, make them suitable to be applied in X-ray imaging applications. Hybrid CMOS^[5,6] and monolithic CMOS^[7] devices have been proposed for soft X-ray imaging spectroscopy in future space astronomy missions.

In this work, a backside-illuminated scientific CMOS (BSI sCMOS), namely, the GSENSE400BSI device developed by Gpixel Inc.^[8], is investigated as an X-ray imaging spectroscopy device. This GSENSE400BSI device can operate near room temperature with an energy resolution of 192 eV at 5.9 keV. The results show that the BSI sCMOS is suitable as the focal plane detector. To meet the requirement of the focal plane detectors of WXT, we will develop a new type of

* lingzhixing@bao.ac.cn; phone 0086 10 64807836;

BSI sCMOS with large size based on the current technology. In this paper, the structure of GSENSE400BSI and its basic characteristics are described in section 2, the experimental setup and results are presented in sections 3 and 4, and conclusions are offered in section 5.

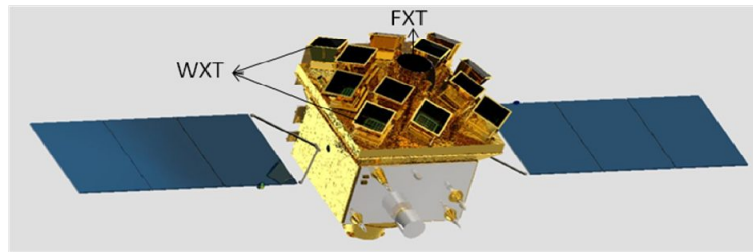


Figure 1: A possible configuration of EP.

2. BSI SCMOS DEVICE

The GSENSE400BSI device is designed for scientific optical applications. Figure 2 shows a photograph and illustration of the physical structure^[9] of this sCMOS device. It has a pixel array of 2048×2048 with a pixel size of 11 μm and an epitaxial depth of 3.6 μm. The pixel design is based on a 4-T pinned photodiode (PPD) structure, as shown in Figure 3(a), which can be combined with correlated double sampling (CDS) for KTC noise and offset cancelling. An HDR transistor is applied for dynamic range enhancement. The pixel operation timing and the bus voltage during the readout of one line are shown in Figure 3(b). The full chip architecture, as shown in Figure 4, is composed of a pixel array, a readout circuit, an SPI interface and a temperature sensor. The image signals from the pixel array are amplified by a column-level programmable gain array (PGA) and digitized by a low-power ADC array^[10]. The digitized image signals are then multiplexed and read out through 8 low-voltage differential signaling (LVDS) channels placed at the bottom of the chip. A more detailed description of the design of this sCMOS can be found in [11]. The BSI sCMOS operates in an electronic rolling shutter mode with a high readout speed. GSENSE400BSI provides three operation modes: high dynamic range image (HDR) mode, low dark current (LDC) mode and standard image (STD) mode. The basic optical properties of the BSI sCMOS are summarized in Table 1^[12].

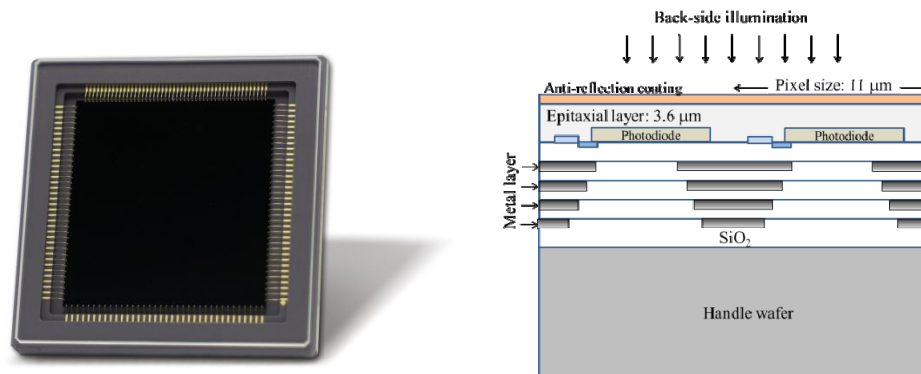


Figure 2: Photograph and physical structure of the BSI sCMOS.

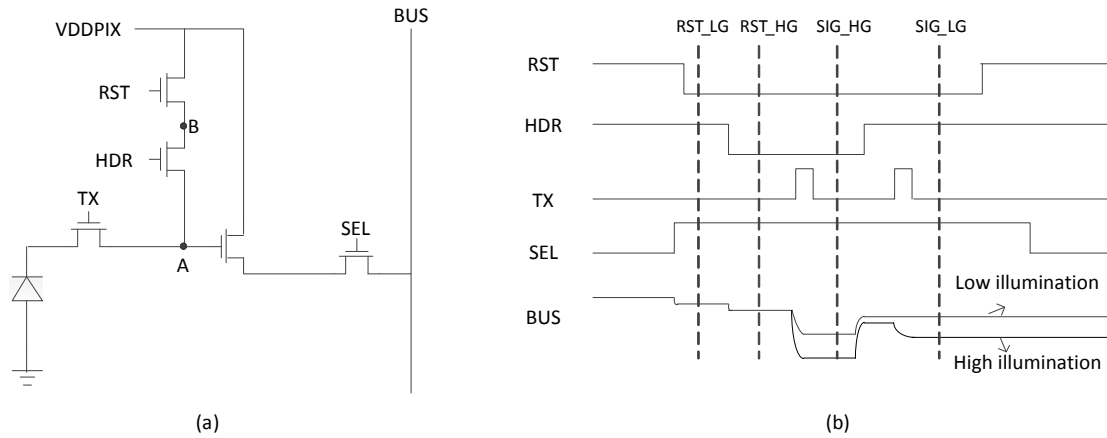


Figure 3: Schematic diagram of a pixel (a) and operation timing (b).

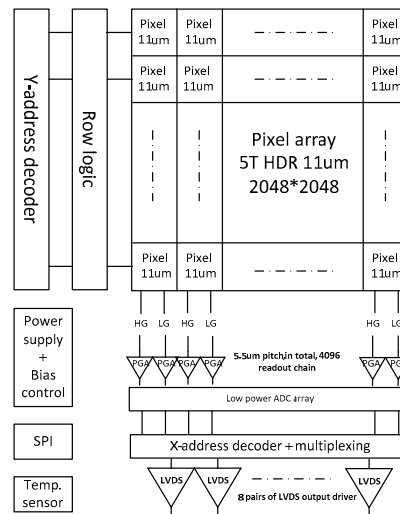


Figure 4: Sensor architecture.

Table 1: Basic properties of the BSI sCMOS.

Pixel size	11 μm
Number of pixels	2048 \times 2048
Epitaxial layer thickness	3.6 μm
Supply voltage	3.3 V (analog)/1.8 V (digital)
Frame rate	48 fps @ STD mode 24 fps @ HDR mode
ADC digit	12 bit
Full well capacity	89 ke-
Power consumption	< 650 mW
Intra-scene dynamic range	> 93 dB
Photo-response non-uniformity (PRNU)	< 1.5%
Fixed pattern noise (FPN)	< 2 e-

3. EXPERIMENTAL SETUP

We use a ^{55}Fe source with 5.9 keV X-ray photons to study the characteristics of this BSI sCMOS detector. The results presented in this paper are obtained in a climate chamber with the temperature controlled between -20°C and 30°C . Figure 5 shows a block diagram of the GSENSE400BSI evaluation system. An evaluation board, which consists of a sensor board and an FPGA board, is used to provide clock and bias voltages for the detector and to perform data transmission. An NI PCIe-1433 frame grabber is used to collect test frames. Considering our interests in soft X-ray energy band, the default setup of the evaluation board with the standard image (STD) mode is used during our test.

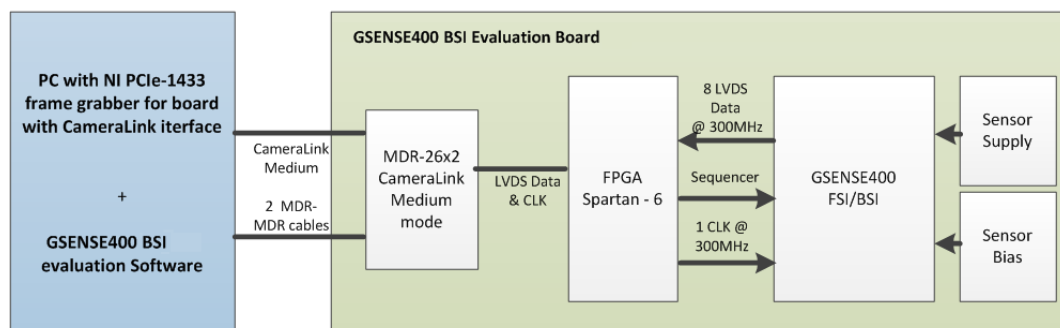


Figure 5. Block diagram of the GSENSE400BSI evaluation system.

4. EXPERIMENTAL RESULTS

4.1 Readout noise

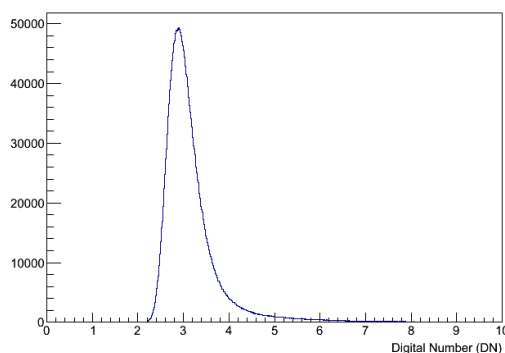


Figure 6: Readout noise at -20°C .

The readout noise is measured by recording 1000 dark frames with the shortest possible integration time ($\sim 15.2 \mu\text{s}$). The pixel-by-pixel standard deviations over these 1000 dark frames are plotted in the histogram shown in Figure 6. The mean determined through Gaussian fitting corresponds to the readout noise. Figure 7 shows the readout noise levels at different temperatures. The readout noise is approximately $1.5 e^-$ ENC (equivalent noise charge) by using the conversion gain $0.53 e^-/\text{DN}$ mentioned in section 4.4.1. There is a slight increase at lower temperatures, which may originate from the interior structure of the pixel. If the selection transistor part of each pixel is cut off, the readout noise of the rest part of pixel decreases with decreasing temperature.

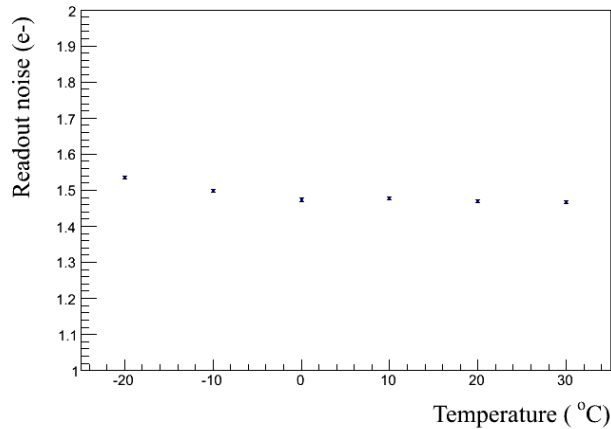


Figure 7: Readout noise as a function of temperature.

4.2 Dark current

Dark current is caused by thermal excitation and is typically overwhelming at room temperature for semiconductor detectors; thus, these detectors need to be cooled to achieve better performance. To evaluate the dark current of this BSI sCMOS, 1000 dark frames are acquired at each of various different integration times, from the shortest possible integration time ($\sim 15.2 \mu\text{s}$) to 0.25 s, at various temperatures. The mean of all pixels in each image is determined, and this value is averaged over these 1000 dark frames for each integration time. Then, a linear fit is performed to find the slope at each temperature, as shown in Figure 8. The slope indicates the dark current at the corresponding temperature. Figure 9 shows the dark currents at a range of temperatures from -20°C to 30°C . The dark current shows no significant reduction below 10°C and is $159 \text{ e}^-/\text{pixel}/\text{s}$ at -20°C . By applying a special working mode, the so-called low dark current (LDC) mode, the dark current can be reduced to less than $1 \text{ e}^-/\text{pixel}/\text{s}$ at -20°C . However, the ratio of splitting events of X-rays will increase due to the electric field change in pixels. New designed sCMOS for WXT may optimize the performance of the dark current as well as the splitting events.

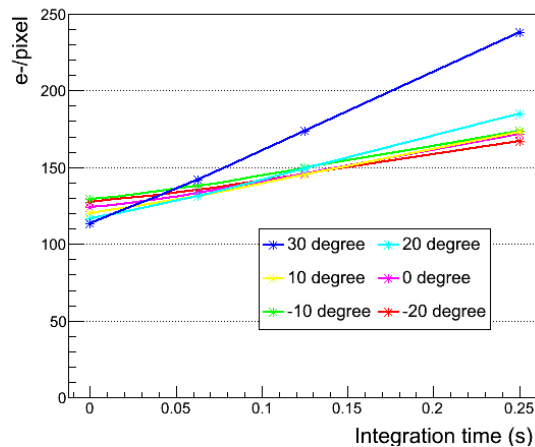


Figure 8: The mean of each image, averaged over 1000 dark frames at each integration time.

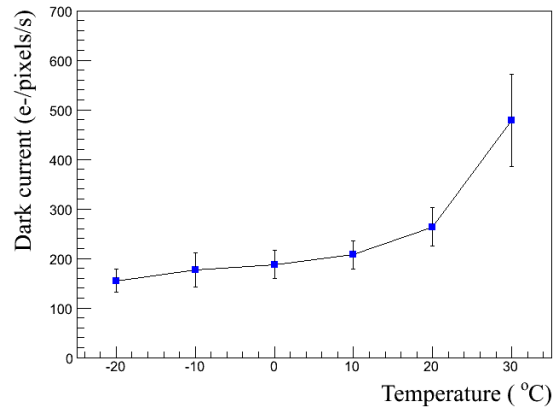


Figure 9: Dark current as a function of temperature.

4.3 X-ray image

To verify that this BSI sCMOS can be used as an X-ray imaging detector, GSENSE400BSI is put in the focal plane position of a so-called lobster-eye type mirror in our X-ray imaging beam line. This beam line, shown in figure 10 (a), is about 14 m and provides a nearly parallel beam with 0-10 keV X-ray. Figure 10 (b) shows the corresponding focused image of the point spread function (PSF) of the MPO by integrating the response of the BSI sCMOS.



Figure 10: (a) X-ray imaging beam line (b) X-ray image captured by GSENSE400BSI.

4.4 Energy response

The basic performance of the BSI sCMOS detector is studied under illumination by a ^{55}Fe X-ray source. The electrons induced by a single X-ray photon may be collected by two or more pixels due to the expansion of the charge cloud; this phenomenon is called a splitting event. The results of each exposure include X-ray signals plus a bias map. The bias map is subtracted before X-ray events selection. All pixels are then scanned for comparison against a threshold of a few times the noise level. All pixels containing a charge greater than this threshold are flagged. If a flagged pixel corresponded to a local maximum in its 3×3 -pixel window and no pixel adjacent in this window is above the threshold, then this event is recorded as a single-pixel event; otherwise it is recorded as a splitting event. The X-ray spectra including all X-ray events and only single-pixel events are shown in Figure 11, respectively. Since the GSENSE400BSI device is not fully-depleted, the single-pixel events are only about 10% of all X-ray events. An almost fully-depleted BSI sCMOS device will be developed for WXT to reduce the fraction of splitting events. For the following section, only single-pixel events are selected for analysis.

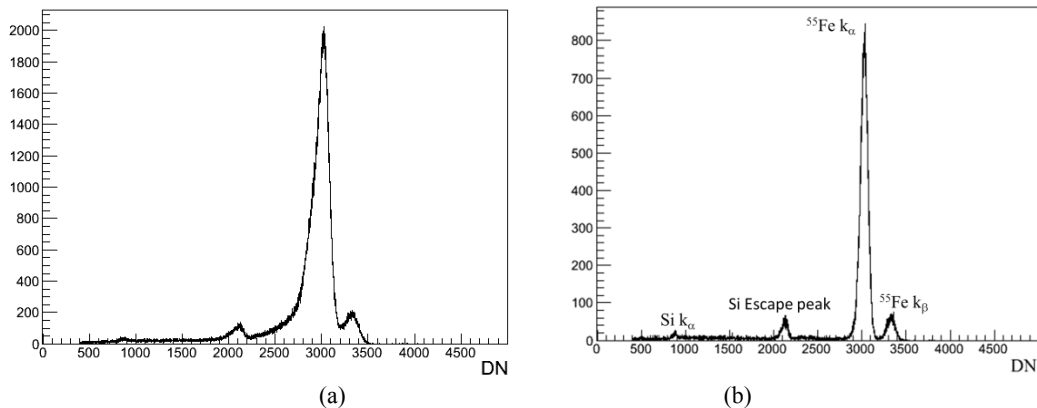


Figure 11: X-ray spectra from the ^{55}Fe source at 20°C (a) all X-ray events (b) only single-pixel events.

4.4.1 Conversion gain

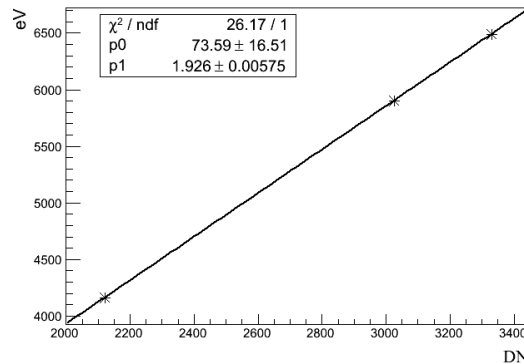


Figure 12: Calibration between the X-ray energy and the output digital number (DN).

The spectrum of the ^{55}Fe source shown in Figure 11 (b) includes the 4.16 keV Si escape line, the 5.9 keV Mn K_α line and the 6.49 keV Mn K_β line. The positions of these lines are obtained through Gaussian fitting. Figure 12 shows the relationship between the incident X-ray energies and the digital numbers obtained as the positions of the X-ray lines. The slope obtained from a linear fit is 1.93 eV/DN, which further indicates a conversion gain of 0.53 e^-/DN , since the mean ionization energy per electron-hole pair is 3.65 eV/ e^- in a Si detector ^[13].

4.4.2 Energy resolution

The energy resolution is an important parameter for an X-ray detector; it determines how well spectral lines can be resolved in observations. A Gaussian function is used to fit the energy spectrum of the Mn K_α peak, and the energy resolution is evaluated as the full width at half maximum (FWHM). Currently, CCDs have a nearly Fano-limited ^[14, 15] energy resolution ($\Delta E/E \sim 2.0\%$ at 5.9 keV).

Using only single-pixel events, the temperature dependence of the energy resolution of the BSI sCMOS detector is evaluated, as shown in Figure 13. Near room temperature (20°C), the energy resolution reaches 192 eV (3.3%) at 5.9 keV. Due to dark current (see Figure 9) which limits the energy resolution at low temperatures, the energy resolution is 187 eV at 5.9 keV at -20°C .

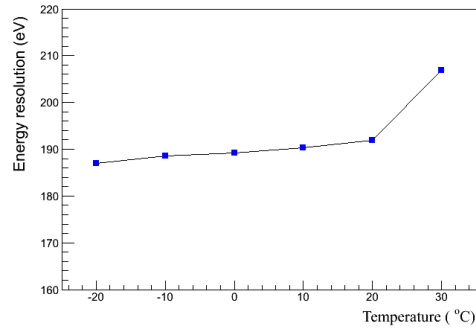


Figure 13: Energy resolutions at different temperatures.

5. CONCLUSIONS

In this work, we studied the characteristics of a BSI sCMOS as an X-ray detector. This BSI sCMOS can operate at room temperature, and the energy resolution reaches 192 eV (3.3%) at 5.9 keV (20°C). When the temperature of the sCMOS devices is cooled down to -20°C, the results showed a readout noise of approximately 1.5 e⁻, a dark current of 159 e⁻/pixel/s, and an energy resolution of 187 eV at 5.9 keV. The dark current limits the energy resolution performance at low temperature. These results show that the BSI sCMOS detector is suitable for application in soft X-ray detection. A more advanced BSI sCMOS prototype with a size of 6×6 cm² and with 10 μm depletion layer has been proposed for the EP mission.

ACKNOWLEDGMENTS

This work is supported by a program of the National Natural Science Foundation of China under Grant No. 11703050, a Young Researcher Grant from the National Astronomical Observatories of the Chinese Academy of Sciences and a Grant from the Key Laboratory of Space Astronomy and Technology, National Astronomical Observatories of the Chinese Academy of Sciences.

REFERENCES

- [1] Angel, J.R.P., "Lobster eyes as X-ray telescopes," *ApJ* 233, 364-373 (1979)
- [2] Bai, Y., Farris, M. C., Joshi, A., and Chuh, T.Y., "Large-format hybrid visible silicon focal plane arrays for space- and ground-based astronomy," *Proc. SPIE* 5499, 151-161 (2004).
- [3] Bai, Y., Bernd, S. G., Hosack, J. R., Farris, M. C., Montroy, and J. T., Bajaj, J., "Hybrid CMOS focal plane array with extended UV and NIR response for space applications," *Proc. SPIE* 5167, 83-93 (2004).
- [4] Bai, Y., Bajaj, J., Beletic, J. W., Joshi, A., and Lauxtermann, S., "Teledyne Imaging Sensors: Silicon CMOS imaging technologies for x-ray, UV, visible and near infrared," *Proc. SPIE* 7021, 702102 (2008).
- [5] Griffith, C.V., Falcone, A. D., Prieskorn, Z. R., Burrows, D. N., "Recent Progress and Development of a Speedster-EXD: a New Event-Triggered Hybrid CMOS X-ray Detector," *Proc. SPIE* 9601, 96010B (2015).

- [6] Hull, S. V., Falcone, A. D., Burrows, D. N., et al. "Recent X-ray hybrid CMOS detector developments and measurements," Proc. SPIE 10397, 1039704 (2017)
- [7] Kenter, A., Kraft, R., Gauron, T., Murray, S. S., "Monolithic CMOS Imaging X-ray Spectrometers," Proc. SPIE 9154, 91540J (2014)
- [8] <http://www.gpixelinc.com/>
- [9] Private communication with the Gpixel Inc Corp.
- [10] Ma, C., Wang, X., "A Low Power Counting Method in Ramp ADCs used in CMOS Image Sensors," in Proc. Int. Image Sensor Workshop, 129-132 (2013)
- [11] Ma, C., Liu, Y., Li, J., Zhou, Q., Chang, Y., Wang, X., "A 4MP high-dynamic-range, low-noise CMOS image sensor," Proc. SPIE 9403, 940305 (2015)
- [12] <http://www.gpixelinc.com/index.php?s=/b/99.html>
- [13] Janesick, J. R., "Scientific Charge-Coupled Devices," SPIE Press, Bellingham, Washington (2001).
- [14] Fano, U., "Ionization Yield of Radiations. II. The Fluctuations of the Number of Ions," Physical Review 72, 26–29 (1947).
- [15] Owens, A., Fraser, G. W., and McCarthy, K. J. "On the experimental determination of the Fano factor in Si at soft X-ray wavelengths," Nuclear Inst & Methods in Physics Research A 491, 437-443 (2002)